

Bounds on length scales of classical spacetime-foam models

S. Bernadotte and F.R. Linkhamer

Institute for Theoretical Physics,
 University of Karlsruhe (TH),
 76128 Karlsruhe, Germany

Abstract

We consider simple models of a classical spacetime foam with identical static defects embedded in Minkowski spacetime. Plane-wave solutions of the vacuum Maxwell equations with appropriate boundary conditions at the defect surfaces are obtained in the long-wavelength limit. The corresponding photon dispersion relations are calculated. In particular, we determine the coefficients of the quadratic and quartic terms in the photon dispersion relation $\omega^2 = \omega^2(\vec{k})$, for angular frequency ω and wave vector \vec{k} . Astrophysical observations of gamma-ray bursts and ultra-high-energy cosmic rays then place bounds on the coefficients of the dispersion relations and, thereby, on particular combinations of the length scales from the static spacetime-foam models considered. Spacetime foam models with a single length scale are excluded, even models with a length scale close to the Planck scale (as long as a classical spacetime manifold remains relevant).

PACS numbers: 04.20.Gz, 41.20.Jb, 11.30.Cp, 98.70.Sa

Keywords: spacetime topology, electromagnetic wave propagation, Lorentz noninvariance, cosmic rays

Electronic address: frans.linkhamer@physik.uni-karlsruhe.de

I. INTRODUCTION

Whether or not space remains smooth down to smaller and smaller distances is an open question. Conservatively, one can say that the typical length scale of any fine-scale structure of space must be less than $10^{-18} \text{ m} = 10^{-3} \text{ fm}$, which corresponds to a center-of-mass energy of 200 GeV in a particle-collider experiment. Astrophysics provides us, of course, with much higher energies, but not with controllable experiments. Still, astrophysics may supply valuable information as long as the relevant physics is well understood.

In this article, we discuss astrophysical bounds solely based on solutions of the Maxwell (and Dirac) equations. These solutions hold for a particular type of classical spacetime manifold with small-scale structure. Specifically, we consider a static (time-independent) structure of space, which is modeled by a homogeneous and isotropic distribution of identical defects embedded in Minkowski spacetime. With appropriate boundary conditions at the defect surfaces, plane-wave solutions of the vacuum Maxwell equations are obtained in the long-wavelength limit. That is, the wavelength must be much larger than $\max(b; l)$, with b the typical size of the individual defect and l the average separation between the different defects. (An analogous problem would be sound propagation in a block of ice with frozen-in bubbles of air.)

Generalizing the terminology of Wheeler and Hawking, we call, in the following, any classical spacetime with nontrivial small-scale structure (resembling bubbly ice, Swiss cheese, or whatever) a "classical spacetime foam" [1, 2, 3, 4, 5, 6]. The plane-wave Maxwell solutions from our classical spacetime-foam models, then, have a modified dispersion relation (angular frequency squared as a function of the wave number $k_{\perp}^2 = \vec{k}_{\perp}^2$):

$$k_{\perp}^2 = a_2^{(1)} c^2 k^2 + a_4^{(1)} b^{(1)} c^2 k^4 + \dots; \quad (1.1)$$

where c is the velocity from the Minkowski line element ($ds^2 = c^2 dt^2 - d\vec{x}^2$), a_2 and a_4 are dimensionless coefficients depending on the length scales of the model (one length scale being b), and j labels different kinds of models.

For simplicity, we consider only three types of defects:

1. a nearly pointlike defect with the interior of a ball removed from \mathbb{R}^3 and antipodal points on its boundary identified;
2. a nearly pointlike defect with the interior of a ball removed from \mathbb{R}^3 and boundary points reflected in a central plane identified;
3. a wormhole-like defect with two balls removed from \mathbb{R}^3 and glued together on their boundaries; cf. Refs. [5, 6].

Further details will be given in Sec. II A. As mentioned above, the spacetime models considered consist of a frozen gas of identical defects (types $j = 1, 2, 3$) distributed homogeneously and isotropically over Euclidean space \mathbb{R}^3 . Note that these classical models are not intended to describe in any detail a possible spacetime-foam structure (which is, most likely, essentially

quantum mechanical in nature) but are meant to provide a simple and clean background for an explicit calculation of potential nonstandard propagation effects of electromagnetic waves.

The type of Maxwell solution found here is reminiscent of the solution from the so-called "Bethe holes" for wave guides [7]. In both cases, the standard Maxwell plane wave is modified by the radiation from fictitious multipoles located in the holes or defects. But there is a crucial difference: for Bethe, the holes are in a material conductor, whereas for us, the defects are "holes" in space itself.

Returning to our spacetime foam models, we also calculate the modified dispersion relation of a free Dirac particle, for definiteness taken to be a proton (mass m_p):

$$\omega_p^2 = a_{p0}^{(0)} m_p^2 c^4 - \omega^2 + a_{p2}^{(0)} c^2 k^2 + a_{p4}^{(0)} b^{(0)2} c^2 k^4 + \dots; \quad (1.2)$$

with dimensionless coefficients a_{p0} , a_{p2} , and a_{p4} . As might perhaps be expected, the response of the Dirac and Maxwell plane waves to the same spacetime foam model turns out to be quite different (in particular, $a_{p2} \neq a_2$). The different proton and photon phase velocities then allow for Cherenkov-type processes [8, 9]. But, also in the pure photon sector, there may be interesting time-dispersion effects [10] as long as the quartic coefficient a_4 of the photon dispersion relation (1.1) is nonvanishing.

In fact, with the model dispersion relations in place, we can use astrophysical observations to put bounds on the various coefficients a_2 and a_4 , and, hence, on particular combinations of the model length scales (e.g., typical defect size b and separation l). Specifically, the absence of time-dispersion of an observed TeV wave from an active galactic nucleus bounds a_4 and the absence of Cherenkov-like effects in ultra-high-energy cosmic rays bounds $a_2 \approx 2$ and a_4 . In other words, astrophysics not only explores the largest structures of space (up to the size of the visible universe at approximately 10^{10} lyr = 10^{26} m) but also the smallest structures (down to 10^{-26} m or less, as will be shown later on).

The outline of the remainder of this article is as follows. In Sec. II, we discuss the calculation of the effective photon dispersion relation from the simplest type of foam model, with static $\epsilon = 1$ defects. The calculations for isotropic $\epsilon = 2$ and $\epsilon = 3$ models are similar and are not discussed in detail (App. A gives additional results for anisotropic defect distributions). Some indications are, however, given for the calculation of the proton dispersion relation from model $\epsilon = 1$ with details relegated to App. B. The main focus of Sec. II and the two appendices is on modified dispersion relations but in Sec. IIIC we also discuss the scattering of an incoming electromagnetic wave by the model defects. In Sec. III, we summarize the different dispersion relations calculated and put the results in a general form. In Sec. IV, this general photon dispersion relation is confronted to the astrophysical observations and bounds on the effective length scales are obtained. In Sec. V, we draw some conclusions for the classical small-scale structure of space and present some further speculations on a hypothetical quantum spacetime foam.

II. CALCULATION

A. Defect types

The present article considers three types of static defects obtained by surgery on the Euclidean 3-space R^3 . The discussion is simplified by initially choosing the origin of the Cartesian coordinates $\mathbf{x} = (x^1; x^2; x^3) = (x; y; z)$ of R^3 to coincide with the "center" of the defect. The corresponding Minkowski spacetime $R = R^3$ has standard metric $(\eta) = \text{diag}(1; -1; -1; -1)$ for coordinates $\mathbf{x} = (x^0; \mathbf{x}) = (ct; \mathbf{x}^m)$ with $m = 0, 1, 2, 3$.

The first type of defect (label $= 1$) is obtained by removing the interior of a ball from R^3 and identifying antipodal points on its boundary (Fig. 1). Denote this ball, its boundary sphere, and point reection by

$$B_b = \mathbf{x} \in R^3 : |\mathbf{x}| \leq b; \quad S_b = \mathbf{x} \in R^3 : |\mathbf{x}| = b; \quad P(\mathbf{x}) = -\mathbf{x}; \quad (2.1)$$

Then, the space manifold with a single defect centered at the origin $\mathbf{x} = 0$ is given by

$$M_b^{[=1]} = M_{0,b}^{[=1]} = \mathbf{x} \in R^3 : |\mathbf{x}| \leq b \wedge (S_b \ni \mathbf{x} = P(\mathbf{x}) \in S_b); \quad (2.2)$$

where \wedge denotes pointwise identification (the 3-space has no boundary) and $M_b^{[=1]}$ is a shorthand notation. The resulting spacetime manifold is $M = R \setminus M_b^{[=1]}$.

The corresponding classical spacetime-foam model is made by a superposition of $= 1$ defects with a homogeneous distribution. The number density of defects is denoted $n \in 1^3$ and only the case of a very rare gas of defects is considered ($b \gg 1$), so that there is no overlap of defects.

For the sake of completeness, let us go through the procedure in more detail. The 3-manifold with $N = 1$ identical defects is given by

$$M_{f\mathbf{x}_1; \dots; \mathbf{x}_N, b}^{[=1]} = M_{\mathbf{x}_1, b}^{[=1]} \setminus M_{\mathbf{x}_2, b}^{[=1]} \setminus \dots \setminus M_{\mathbf{x}_N, b}^{[=1]}, \quad (2.3)$$

where $M_{\mathbf{x}_n, b}^{[=1]}$ is the single-defect manifold (2.2) with the origin of the sphere moved from $\mathbf{x} = 0$ to $\mathbf{x} = \mathbf{x}_n$ and the minimum distance between the different centers \mathbf{x}_n is assumed to be larger than $2b$. The final spacetime-foam manifold takes the Cartesian product of R with the $N = 1$ "limit" of (2.3),

$$M_{\text{distribution}, b}^{[=1]} = R \times \lim_{N \rightarrow 1} M_{f\mathbf{x}_1; \dots; \mathbf{x}_N, b}^{[=1]}; \quad (2.4)$$

where one needs to describe the statistical distribution of the centers \mathbf{x}_n . As mentioned above, we take the simplest possible distribution, homogeneous, and the only quantity to specify is the number density n of defects.

The second type of defect ($= 2$) follows by the same construction, except that the identified points of the sphere S_b are obtained by reection in an equatorial plane with unit normal vector \mathbf{b} (Fig. 2). For a point \mathbf{x} on the sphere S_b , the reected point is denoted $R_b(\mathbf{x})$. With a single defect present, global Cartesian coordinates can be chosen so that \mathbf{b}

points in the 3{direction and $(x^1; x^2; x^3) \in S_b$ is to be identified with $(x^1; x^2; -x^3) \in S_b$.] The space with a single $\kappa = 2$ defect centered at the origin $\mathbf{x} = 0$ (not indicated by our shorthand notation) is then given by

$$M_{b;b}^{[\kappa=2]} = \mathbf{x} \in \mathbb{R}^3 : \dot{\mathbf{x}} \cdot \mathbf{b} \wedge (S_b \ni \mathbf{x} = R_b(\mathbf{x}) \in S_b) ; \quad (2.5)$$

and spacetime is $R = M_{b;b}^{[\kappa=2]}$. Strictly speaking, the 3{space (2.5) is not a manifold but an orbifold [11], i.e., a coset space $M = G$, for manifold M and discrete symmetry group G . This 3{space has, in fact, singular points corresponding to the fixed points of R_b , which lie on the great circle of S_b in the equatorial plane with normal vector \mathbf{b} . But away from these singular points, this 3{space is a genuine manifold and we simply use the (slightly misleading) notation M in (2.5). The corresponding classical spacetime-foam model results from a homogeneous and isotropic (randomly oriented) distribution of $\kappa = 2$ defects.

The third type of defect ($\kappa = 3$) results from a somewhat more extensive surgery [5, 6]. Now, the interiors of two identical balls are removed from \mathbb{R}^3 . These balls, denoted B_b and B_b^0 , have their centers separated by a distance $d > 2b$. The two boundary spheres S_b and S_b^0 are then pointwise identified by reection in the central plane (Fig. 3). This reection is again denoted R_b . [With ball centers at $\mathbf{x} = (d/2, 0, 0)$, the reection plane is simply given by $x^1 = 0$.] The space manifold with a single $\kappa = 3$ defect centered at the origin $\mathbf{x} = 0$ is now

$$M_{b;b;d}^{[\kappa=3]} = \mathbf{x} \in \mathbb{R}^3 : \dot{\mathbf{x}} \cdot (d/2) \mathbf{b} \wedge \mathbf{j} \wedge \dot{\mathbf{x}} + (d/2) \mathbf{b} \wedge \mathbf{j} \wedge \mathbf{b} \wedge (S^3 \ni \mathbf{x} = R_b(\mathbf{x}) \in S_b^0) ; \quad (2.6)$$

and the spacetime manifold is $R = M_{b;b;d}^{[\kappa=3]}$. Again, the corresponding classical spacetime-foam model results from a homogeneous and isotropic distribution of $\kappa = 3$ defects.

For later use, we also define a $\kappa = 3^0$ defect with distance d fixed to the value $4b$. An individual $\kappa = 3^0$ defect then has only one length scale, b , which simplifies some of the discussion later on. The relevant space manifold is thus

$$M_{b;b}^{[\kappa=3^0]} = M_{b;b;4b}^{[\kappa=3]} ; \quad (2.7)$$

with the $\kappa = 3$ manifold defined by (2.6).

Let us end this subsection with two technical remarks, one mathematical and one physical. First, the $\kappa = 1$ and $\kappa = 3$ space manifolds are multiply connected (i.e., have noncontractible loops) but not the $\kappa = 2$ space. Second, the classical spacetimes considered in this article do not solve the vacuum Einstein equations but appear to require some exotic form of energy located at the defects; see, e.g., Part III of Ref. [6] for further discussion.

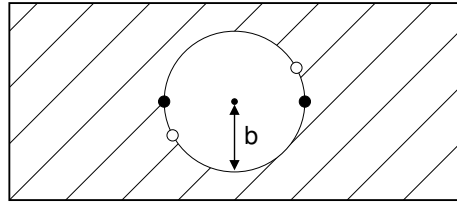


FIG. 1: Space manifold (2.2) from a single spherical defect (type = 1, radius b) embedded in \mathbb{R}^3 with its 'interior' removed and antipodal points identified (as indicated by the pairs of open and filled circles). The corresponding classical spacetime foam model has a homogeneous distribution of static = 1 defects.

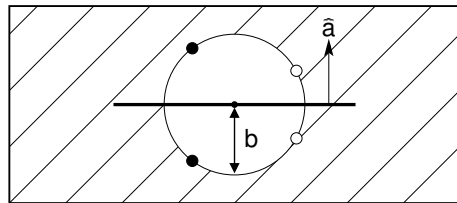


FIG. 2: Space manifold (2.5) from a single spherical defect (type = 2, radius b) embedded in \mathbb{R}^3 with its 'interior' removed and points identified by reflection in the equatorial plane with normal vector \mathbf{a} . The corresponding classical spacetime foam model has a homogeneous and isotropic distribution of static = 2 defects.

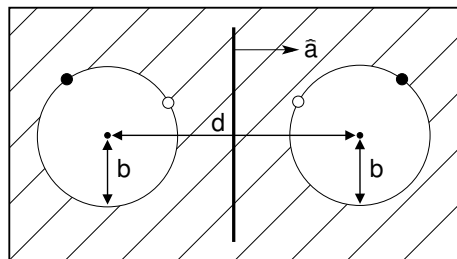


FIG. 3: Space manifold (2.6) from a single wormhole-like defect (type = 3, two spheres with radii b and distance d between the centers) embedded in \mathbb{R}^3 with the 'interiors' of the two spheres removed and their points identified by reflection in the central plane with normal vector \mathbf{a} . The corresponding classical spacetime foam model has a homogeneous and isotropic distribution of static = 3 defects.

B. Photon dispersion relation

The task, now, is to determine the electromagnetic wave properties for the three types of classical spacetime-foam models considered. The $\epsilon = 1$ case will be discussed in some detail but not the other cases, for which only results will be given.

The calculation is relatively straightforward and consists of three steps. First, start from the standard plane-wave solution of the vacuum Maxwell equations,

$$\mathbf{E}_0(\mathbf{x};t) = E_0 \hat{\mathbf{x}} \exp(kz - it); \quad \mathbf{B}_0(\mathbf{x};t) = E_0 \hat{\mathbf{y}} \exp(kz - it); \quad (2.8)$$

which corresponds to a linearly polarized plane wave propagating in the $\mathbf{z} \equiv \mathbf{x}^3$ direction ($\hat{\mathbf{x}}$ and $\hat{\mathbf{y}}$ are unit vectors pointing in the \mathbf{x}^1 and \mathbf{x}^2 directions, respectively). The electromagnetic fields (2.8) provide a valid solution of the Maxwell equations between the "holes" of the manifold, as given by (2.4) for $\epsilon = 1$ defects.

Second, add appropriate vacuum solutions $(\mathbf{E}_1; \mathbf{B}_1)$, so that the total electric and magnetic fields, $\mathbf{E}_{\text{total}} = \mathbf{E}_0 + \mathbf{E}_1$ and $\mathbf{B}_{\text{total}} = \mathbf{B}_0 + \mathbf{B}_1$, satisfy the boundary conditions from a single defect. The boundary conditions for the electric field (polar vector \mathbf{E}) at the defect surface follow simply by considering the allowed motions of a test particle (see, for example, the points marked in Fig. 1 for tangential motion), whereas the magnetic field (axial vector \mathbf{B}) has the "opposite" behavior. In fact, it suffices to consider the behavior of the electric field \mathbf{E} near the defect since the magnetic field \mathbf{B} is orthogonal to it by the vacuum Maxwell equations.

Third, sum over the contributions of the different defects from the spacetime-foam model and obtain the effective dielectric and magnetic permittivities, ϵ and μ , which may be wavelength dependent. The dispersion relation for the isotropic case is then given by

$$\omega^2(k) = c^2 k^2 = \epsilon(k) \mu(k); \quad (2.9)$$

and we refer the reader to the textbooks for further discussion; see, e.g., Secs. 7.5(a) and 9.5(d) of Ref. [12] and Sec. II{32} of Ref. [13].

The specifics of the second and third step of the calculation for $\epsilon = 1$ defects are as follows. In step 2, the boundary conditions at the surface S_b of manifold (2.2) are:

$$\mathbf{b}(\mathbf{x}) \cdot \mathbf{E}(\mathbf{x};t) = \mathbf{b}(\mathbf{x}) \cdot \mathbf{E}(\mathbf{x};t); \quad \mathbf{b}(\mathbf{x}) \cdot \mathbf{E}(\mathbf{x};t) = +\mathbf{b}(\mathbf{x}) \cdot \mathbf{E}(\mathbf{x};t) \quad [=\epsilon]; \quad (2.10a)$$

$$\mathbf{b}(\mathbf{x}) \cdot \mathbf{B}(\mathbf{x};t) = +\mathbf{b}(\mathbf{x}) \cdot \mathbf{B}(\mathbf{x};t); \quad \mathbf{b}(\mathbf{x}) \cdot \mathbf{B}(\mathbf{x};t) = -\mathbf{b}(\mathbf{x}) \cdot \mathbf{B}(\mathbf{x};t) \quad [=\mu]; \quad (2.10b)$$

where $\mathbf{b}(\mathbf{x})$ is the outward unit normal vector of the surface at point $\mathbf{x} \in S_b \subset \mathbb{R}^3$. Clearly, constant fields $\mathbf{E} / E_0 \hat{\mathbf{x}}$ and $\mathbf{B} / B_0 \hat{\mathbf{y}}$, corresponding to the unperturbed fields (2.8) over length scales of order b , do not satisfy the defect boundary conditions (2.10) and need to be corrected. As discussed in the Introduction, the correction fields \mathbf{E}_1 and \mathbf{B}_1 correspond to multipole fields from "mirror charges" located at the center of the individual defect. The leading contributions of a $\epsilon = 1$ defect come from fictitious electric and magnetic dipoles

at the defect center, each aligned with their respective initial elds (2.8) and both with a strength proportional to $b^3 E_0$. For $\epsilon = 1$ and $kb \ll 1$, the electric eld E_{total} turns out to be normal to the surface S_b and the magnetic eld B_{total} tangential, just as for a perfectly conducting sphere (see, e.g., Secs. 13.1 and 13.9 of Ref. [14]).

In step 3 of the calculation for $\epsilon = 1$ defects, the effective dielectric and magnetic permeabilities (Gaussian units) are found to be given by

$$[\epsilon = 1] \quad 1 + 4 nb^3 j_0(kb) + j_2(kb) ; \quad (2.11a)$$

$$[\epsilon = 1] \quad 1 - 2 nb^3 j_0(kb) + j_2(kb) ; \quad (2.11b)$$

where $n = 1/l$ is the number density of defects (average separation l) and $j_p(z)$ is the spherical Bessel function of order p , for example, $j_0(z) = (\sin z)/z$. The similarity signs in Eqs. (2.11a) and (2.11b) indicate that only the $\epsilon = 1$ multipoles have been taken into account [15]. With (2.9), the dispersion relation is then

$$[\epsilon = 1](k)^2 = \frac{c^2 k^2}{1 + 4 nb^3 [j_0(kb) + j_2(kb)] - 1 - 2 nb^3 [j_0(kb) + j_2(kb)]} ; \quad (2.12)$$

which is valid for $kb \ll 1$. A Taylor expansion in nb^3 and kb gives

$$[\epsilon = 1](k)^2 = 1 - 2 nb^3 c^2 k^2 + (= 5) nb^5 c^2 k^4 + \dots : \quad (2.13)$$

As mentioned above, the dispersion relation (2.12) has been derived for small enough values of k . However, taking this expression (2.12) at face value, we note that the corresponding front velocity ($v_{\text{front}} = \lim_{k \rightarrow 1} v_{\text{phase}}$) would be precisely c . (See, e.g., Ref. [16] for the relevance of the front velocity to the important issues of signal propagation and causality.)

For the $\epsilon = 2$ spacetime-foam model, the dispersion relation is found to be given by

$$[\epsilon = 2](k)^2 = \frac{c^2 k^2}{1 + 2 nb^3 j_0(kb) + j_2(kb)} ; \quad (2.14)$$

with Taylor expansion

$$[\epsilon = 2](k)^2 = 1 - 2 nb^3 c^2 k^2 + (= 5) nb^5 c^2 k^4 + \dots : \quad (2.15)$$

The result (2.15) for randomly orientated $\epsilon = 2$ defects agrees, to the order shown, with the previous result (2.13) for unoriented $\epsilon = 1$ defects. Some results for anisotropic defect distributions are given in App. A.

For the $\epsilon = 3$ case, the calculation is more complicated and we have to work directly with Taylor expansions, keeping only the leading order terms in $b=d$. The end result is

$$[\epsilon = 3](k)^2 = 1 - (20 - 3) nb^3 c^2 k^2 + (2 - 9) nb^3 d^2 c^2 k^4 + \dots ; \quad (2.16)$$

which holds for $kb \ll kd \ll 1$. For anisotropic defect distributions, some results are again given in App. A.

C . Scattering

In this subsection, another aspect of electromagnetic-wave propagation is discussed, namely the scattering of an incoming wave by $\epsilon = 1$ defects. Similar results are expected for $\epsilon = 2$ and $\epsilon = 3$ defects.

As mentioned in Sec. II A, the boundary conditions of a $\epsilon = 1$ defect correspond precisely to those of a perfectly conducting sphere. So the problem to consider is the scattering of electromagnetic waves by a random distribution of identical perfectly conducting spheres with radii b and average separation l , in the long-wavelength limit. More precisely, the case of interest has $b \ll l$, whereas ideal Rayleigh scattering (incoherent scattering by randomly distributed dipole scatterers) would have $b \ll \ll l$; see, e.g., Secs. 9.6 and 9.7 of Ref. [12] and Sec. I{32{5 of Ref. [13]. This means that all of our dipoles in a volume k^3 radiate coherently and their number, $N_{coh} \propto k^3 = l^3$, appears as an extra numerical factor in the absorption coefficient compared to Rayleigh scattering.

The relevant absorption coefficient (inverse scattering length) is then given by

$$[\epsilon = 1] \quad \kappa = \kappa_{scatt}^{[\epsilon = 1]} \propto \frac{1}{dip} l^{-3} N_{coh}; \quad (2.17)$$

with κ_{dip} the cross section from the electric/magnetic dipole corresponding to an individual defect, l^{-3} the number density of such dipoles (i.e., defects), and $N_{coh} \propto 1$ the coherence factor for the $\epsilon = 1$ case discussed above. From the calculated polarizabilities of a $\epsilon = 1$ defect, one has $\kappa_{dip} \propto k^4 b^6$ neglecting factors of order unity. With $N_{coh} \propto (k l)^3$, the scattering length becomes

$$L_{scatt}^{[\epsilon = 1]} \propto k^{-1} l^{-1} b^{-6}; \quad (2.18)$$

up to factors of order unity. Expression (2.18) suffices for our purpose but can, in principle, be calculated exactly, given the statistical distribution of defects.

D . Proton dispersion relation

In this subsection, we obtain the dispersion relations from the Klein-Gordon and Dirac equations for the $\epsilon = 1$ spacetime-foam model. Similar results are expected for the $\epsilon = 2$ and $\epsilon = 3$ models.

For $\epsilon = 1$ defects and the long-wavelength approximation $kb \ll 1$ (i.e., considering the undisturbed harmonic fields to be spatially constant on the scale of the defect), the heuristics is as follows:

a scalar field obeying the Klein-Gordon equation does not require additional sources to satisfy the boundary conditions at $x^j = b$ and, therefore, the dispersion relation is unchanged to leading order (there may, however, be other effects such as scattering [17]);

a spinor field obeying the Dirac equation does require additional sources but their monopole-like contributions average to zero for many randomly positioned defects and the dispersion relation is unchanged to leading order.

A detailed calculation (not reproduced here) gives, indeed, unchanged constant and quadratic terms in the dispersion relation of a real scalar, at least to leading order in kb . The Dirac calculation is somewhat more subtle and details are given in App. B. The end result for the dispersion relation of a free Dirac particle, for definiteness taken to be a proton, is:

$$!_{\text{p}}^{[=1]}(k)^2 = m_{\text{p}}^2 c^4 -^2 + c^2 k^2 + \dots; \quad (2.19)$$

with higher-order terms neglected and proton mass m_{p} . These neglected higher-order terms would, for example, arise from additional factors $k^2 b^2$ and $b^2 = l^2$, resulting in possible terms with the structure $c^2 k^2 m_{\text{p}}^2 c^2 -^2 b^4 = l^4$ and $c^2 k^4 b^4 = l^4$.

The combined photon and proton dispersion relation results will be discussed further in the next section.

III. DISPERSION RELATION RESULTS

A. Coefficients

The different dispersion relations encountered up till now can be summarized as follows:

$$!_{\text{s}}^{[=1]}(k)^2 = m_{\text{s}}^2 c^4 -^2 + 1 + K_{\text{s} \ 2} b^3 = l^3 c^2 k^2 + K_{\text{s} \ 4} b^5 = l^5 c^2 k^4 + \dots; \quad (3.1)$$

for defect type $s = 1, 2, 3$ and species $s = \text{p}, \text{e}$, p corresponding to the Maxwell, Klein-Gordon, and Dirac equations, respectively. Four remarks are in order. First, the implicit assumption of (3.1) is that all particles have the same maximum limiting velocity c in the absence of defects. Second, the photon mass vanishes in Maxwell theory, $m = 0$, as long as gauge invariance holds. Third, only a few coefficients have been shown explicitly in (3.1) and, a priori, there may be many more (even up to order k^4 , as explained at the end of Sec. II D). Fourth, we have added, for clarity, a suffix on the length scales b and l of the models, since the scale b of a $= 1$ defect, for example, is not the same quantity as the scale b of a $= 3$ defect. But, elsewhere in the text, we omit this suffix, as long as it is clear which model is discussed.

In the previous section, we have calculated the photon coefficients $K_{\text{p}2}$ and $K_{\text{p}4}$ for all three foam models ($s = 1, 2, 3$), but those of the scalar and proton dispersion relations only for the $s = 1$ model. The quadratic and quartic photon coefficients are given in Table I. The quadratic proton coefficient $K_{\text{p}12}$ vanishes according to Eq. (2.19), as does the scalar coefficient $K_{\text{e}12}$.

Remark that the calculated dispersion relations (3.1) do not contain cubic terms in k , consistent with general arguments based on coordinate independence and rotational invariance

TABLE I: Coefficients K in the photon dispersion relation (3.1), for $s = 0$, $m^2 = 0$, and defect type .

	K_2	K_4
$= 1$	2	$= 5$
$= 2$	2	$= 5$
$= 3$	$20 = 3$	$(2 = 9) d^2 = b^2$

[18]. Furthermore, the photon dispersion relations found are the same for both polarization modes (i.e., absence of birefringence). For an anisotropic distribution of defects of type $= 2$ or $= 3$, however, the photon dispersion relations do show birefringence but still no cubic term s ; see App. A .

B . General form

The previous results on the dispersion relation (3.1) for the proton and photon can be combined and rewritten in the following general form :

$$!_p^2 = \bar{m}_p^2 c_p^4 = \bar{c}_p^2 k^2 + O(k^4); \quad (3.2a)$$

$$!^2 = 1 + \bar{b} \bar{l} \bar{l} c_p^2 k^2 + \bar{b} \bar{l} \bar{l} c_p^2 k^4 + \dots; \quad (3.2b)$$

for $0 \leq \bar{k} b; \bar{k} l \leq 1$ and with on/o factors $\bar{b}; \bar{l}$ f $1; 0; + 1g$. The velocity squared \bar{c}_p^2 is defined as the coefficient of the quadratic term in the proton dispersion relation (3.2a) and the effective proton mass squared \bar{m}_p^2 is to be identified with the experimental value.

With the results of Table I and Eq. (2.19), it is easy to get the explicit expressions for the effective length scales \bar{b} and \bar{l} in terms of the fundamental length scales b and l of the spacetime model considered. Specifically, the $= 1$ spacetime foam model gives

$$= 1 : \bar{b} = 10^{1/2} b_1; \bar{l} = (2)^{1/3} 10^{1/2} l_1; \bar{b} = 1; \bar{l} = 1; \quad (3.3)$$

with radius b_1 of the individual defects (empty spheres with antipodal points identified) and average separation l_1 between the different defects. Similar results are expected for the $= 2$ and $= 3$ models, defined by Eqs. (2.5) and (2.7), respectively. More generally, one could have a mixture of different defects (types $= 1; 2; 3$ or other), with calculable parameters \bar{b} , \bar{l} , and $\bar{b}_{2,4}$ in the photon dispersion relation (3.2b).

For the purpose of this article, the most important result is that the effective length scales \bar{b} and \bar{l} of the photon dispersion relation (3.2b) are directly related to the fundamental length scales of the underlying spacetime model. This is a crucial improvement compared to a previous calculation of anomalous effects from a classical spacetime foam [19, 20], where the connection between effective and fundamental length scales could not be established rigorously.

The parametrization (3.2), which holds true in general, will be used in the following. Moreover, a $\bar{b}=\bar{l}$ ratio of order one will be allowed for, even though the calculations of Sec. II B, leading for example to the identifications (3.3), are only valid under the technical assumption $b=l$. In short, the proposal is to consider a modest generalization of our explicit results.

IV. ASTROPHYSICAL BOUNDS

The discussion of this section closely follows the one of some previous articles [20, 21, 22], which investigated modified dispersion relations from an entirely different (and less general [23]) origin. For completeness, we repeat the essential steps and give the original references. Note also that, for simplicity, we focus on two particular "gold-plated" events but that other astrophysical input may very well improve the bounds obtained here.

A. Time-dispersion bound

The starting point for our first bound is the suggestion [10] that the absence of dispersion in a highly energetic burst of gamma rays can be used to obtain limits on modified dispersion relations (see, e.g., Refs. [24, 25] for subsequent papers and Ref. [26] for a recent review).

From the photon dispersion relation (3.2b), the relative change of the group velocity v_g $\Delta v_g = v_g(k_2) - v_g(k_1)$ between two different wave numbers k_1 and k_2 is given by [27]:

$$\frac{c}{c} \frac{v_g(k_1) - v_g(k_2)}{v_g(k_1)} \quad (3.2) \quad k_1^2 - k_2^2 \bar{b} = \bar{l}^3; \quad (4.1)$$

where $c=c$ on the left-hand side is a convenient short-hand notation and where \bar{b} and \bar{l} on the right-hand side can be interpreted as the typical defect size and separation, respectively (see Sec. II B for further discussion). A flare of duration t from a source at distance D , with wave-number range $k_1 - k_2 = k_{\text{max}} - k_{\text{min}} = E_{\text{max}}/c = (\sim c)$, constrains the relative change of group velocity, $\Delta v_g = v_g(k_2) - v_g(k_1) \approx c t/D$, which results in the following bound:

$$\bar{b} = \frac{1}{3} \frac{c t}{E_{\text{max}}} \quad (4.2) \quad \begin{aligned} & \bar{b} = \frac{1}{3} \frac{c t}{E_{\text{max}}} \quad \frac{c t}{D}^{1/2} \\ & 1.3 \quad 10^{26} \text{ m} \quad \frac{2.0 \text{ TeV}}{E_{\text{max}}} \quad \frac{t}{280 \text{ s}}^{1/2} \quad \frac{1:1}{D=c} \quad 10^6 \text{ s}^{1/2} \end{aligned}$$

With values inserted for a TeV gamma ray are from the active galactic nucleus Mkn 421 observed on May 15, 1996, at the Whipple Observatory [28]. The scheduled Gamma-ray Large Area Space Telescope (GLAST) may improve this bound by a factor of 10^4 , as discussed in App. A of Ref. [22].

B . Scattering bound

It is also possible to obtain an upper limit on the ratio \bar{b}/\bar{l} by demanding the scattering length L to be larger than the source distance D or, better, larger than $D = 100$ for an allowed reduction of the intensity by a factor $F = \exp(f) = \exp(100)$. In other words, the chance for a gamma-ray to travel over a distance D would be essentially zero if L were less than $D = 10^2$ (see discussion below).

The relevant expression for the scattering length L from $= 1$ defects has been given in Sec. II C . Here, we simply replace b and l in result (2.18) by the general parameters \bar{b} and \bar{l} , again allowing for the case $\bar{b} \ll 1$. Demanding $L > D = f$, then gives the announced bound:

$$\bar{b}/\bar{l}^3 < \frac{P}{f} \left(k_{\text{max}} D \right)^{1/2}$$

$$1.7 \quad 10^{21} \quad \frac{f}{10^2}^{1/2} \quad \frac{2.0 \text{ TeV}}{E_{\text{max}}}^{1/2} \quad \frac{3.3}{D} \quad 10^4 \text{ m}^{1/2}; \quad (4.3)$$

where we have used the same notation and numerical values as in (4.2) and where $f = 1$ corresponds to an allowed reduction of the intensity by f e-foldings.

Strictly speaking, bound (4.3) is useless if f is left unspecified. The problem is to decide, given a particular source, which intensity-reduction factor $F = \exp(f)$ is needed to be sure that its gamma-rays would not reach us if L were less than $D = f$. Practically speaking, we think that a factor $F = \exp(100)$ is already sufficient, but the reader can make up his or her own mind. More important for bound (4.3) to make sense is that one must be certain of the source of the observed gamma-rays and, thereby, of the distance D . For the particular TeV gamma-ray discussed here, the identification of the source as Mkn 421 appears to be reasonably firm [28],

C . Cherenkov bounds

An entirely different type of constraint follows from the observation [8, 9] that ultra-high-energy cosmic rays (UHECRs) can be used to restrict possible Lorentz-noninvariance effects (or possible effects from a violation of the equivalence principle).

From a highly energetic cosmic-ray event observed on October 15, 1991, by the Fly's Eye Air Shower Detector [29, 30], Gagnon and Moore [31] have obtained the following bounds [32]:

$$3 \quad 10^{23} < \bar{b}_2 \bar{l}^3 < 3 \quad 10^{23}; \quad (4.4a)$$

$$7 \quad 10^{39} \text{ m}^2 < \bar{b}_4 \bar{l}^3 < 5 \quad 10^{38} \text{ m}^2; \quad (4.4b)$$

for scale parameters \bar{b} , \bar{l} and sign factors \bar{b}_2 , \bar{b}_4 defined by dispersion relations (3.2a) and (3.2b). Here, the primary was assumed to be a proton with energy $E_p^{\text{UHECR}} = 3 \times 10^{11} \text{ GeV}$ and standard partonic distributions. Note that the limits of bounds (4.4a) and (4.4b) scale approximately as $3 \times 10^{11} \text{ GeV} = E_p^{\text{UHECR}}^n$ with $n = n_a = 2$ and $n = n_b = 4$, respectively.

See Ref. [31] for further details on these bounds and App. B of Ref. [22] for a heuristic discussion.

V. CONCLUSIONS

The time-dispersion bound (4.2) on a particular combination of length scales is direct and, therefore, reliable. The same holds for the scattering bound (4.3), as long as the allowed intensity-reduction factor is specified (see Sec. IV B for further discussion). The Cherenkov bounds (4.4a) and (4.4b), however, are indirect in that they depend on further assumptions (e.g., interactions described by quantum electrodynamics and standard-model partonic structure of the primary hadron). Still, the physics involved is well understood and, therefore, these Cherenkov bounds can be considered to be quite reliable [33].

It is well known (and already realized by Friedmann [34]) that there is no real understanding of what determines the large-scale topology of space. With the advent of quantum theory, a similar lack of understanding (discussed, in particular, by Wheeler [2]) applies to the small-scale structure of space. Even so, assuming the relevance of a classical spacetime-foam model (see discussion below), Occam's razor suggests the model to have a single length scale, with characteristic defect size \bar{b} and average separation \bar{l} of the same order, $\bar{b} \sim \bar{l}$. Without natural explanation, it would be hard to understand why the defect gas would be extremely rare, $\bar{b} \ll \bar{l}$. In the following discussion, we focus on the single-length-scale case but the alternative (rare gas) case should be kept in mind.

According to the time-dispersion limit (4.2), a static classical spacetime foam with a single length scale must have

$$\bar{l}^{\text{single-scale}} < 10^{-26} \text{ m} \quad 2 \quad 10^0 \text{ GeV} = (\sim c)^{-1}; \quad (5.1)$$

which is a remarkable bound compared to what can be achieved by particle-collider experiments on Earth. As mentioned in Sec. IV A, the experimental limit (5.1) may even be improved by a factor 10^4 in the near future, down to a value of the order of 10^{-30} m .

But the scattering and Cherenkov bounds (4.3) and (4.4a) lead to a much stronger conclusion: within the validity of the model, these bounds rule out a single-scale classical spacetime foam altogether [35],

$$\bar{b} = 0(1); \quad (5.2)$$

The fact that a single-scale static foam model is unacceptable holds even for values of $\bar{b} \sim \bar{l}$ down to some $10^{-33} \text{ m} \sim 10^{-16} \text{ m}_{\text{Planck}}$, at which scale a classical spacetime manifold may still have some relevance for describing physical processes (the definition of l_{Planck} will be given shortly).

The result (5.2) applies, strictly speaking, only to the static single-scale foam models considered. But we do expect this conclusion to hold more generally, for example, for the case of a time-dependent small-scale structure, as long as the typical time scale \bar{t} of the spacetime foam is also determined by the hypothesized single scale, $\bar{t} \sim \bar{l} = c$ [36].

At lengths of the order of the Planck scale, $l_{\text{Planck}} \stackrel{P}{\sim} \frac{c}{G} \sim 10^{35} \text{ m}$, it is not clear what sense to make of a classical spacetime picture [37]. Still, at lengths of order $10^2 l_{\text{Planck}}$, for example, one does expect a classical framework to emerge and, then, our results indicate that the effective classical spacetime in an ifold is remarkably smooth ($\delta = 10^{-8}$) [41]. If this conclusion is born out, it would suggest that either the fluctuations of the quantum spacetime foam at the Planck length scale [1, 2, 3, 4] are somehow made ineffective on larger scales or there is no quantum spacetime foam in the first place.

ACKNOWLEDGMENTS

The authors are grateful to K. Busch, D. Hardtke, C. Kaufhold, C. Rupp, and G.E. Volovik for helpful discussions.

APPENDIX A: BIREFRINGENCE

The individual defects of type $\ell = 2$ and $\ell = 3$ have a preferred direction given by the unit vector \mathbf{b} in Figs. 2 and 3, respectively. An anisotropic distribution of defects may then lead to new effects compared to the case of isotropic distributions considered in the main text. This appendix presents some results for the photon dispersion relations from aligned $\ell = 2$ and $\ell = 3$ defects.

For a highly anisotropic distribution of perfectly aligned $\ell = 2$ defects (empty spheres with points reflected in an equatorial plane identified), the two photon polarization modes have different dispersion relations:

$$!^{[\ell=2]} k_{jj}^2 = \frac{k^6 + 6 k^2 (k_{jj}^2 - 2k_z^2) h(kb) nb c^2 k^2}{k^2 + 6 h(kb) nb^2 k^2 - 12 h(kb) nb} ; \quad (\text{A 1a})$$

$$!^{[\ell=2]} k_{jj}^2 = \frac{k^6 + 6 k^2 (k_z^2 - 2k_{jj}^2) h(kb) nb c^2 k^2}{k^2 + 6 h(kb) nb^2 k^2 - 12 h(kb) nb} ; \quad (\text{A 1b})$$

with auxiliary function $h(z) = \cos z / (\sin z) = z$ and definitions for the parallel wave number k_{jj} & k_z , the perpendicular wave number k & k_z , the defect number density n & $1 = 1$. For generic wave numbers $k_{jj} \neq k_z$, the two polarization modes have different phase velocities ($v_{\text{phase}} = k \neq k_z$) and there is birefringence.

For perfectly aligned $\ell = 3$ defects (worm hole-like defects with two empty spheres identified), we do not have a closed expression for the dispersion relations of the two polarization modes but rather Taylor series (the case considered has $kb = kd = kl = 1$). Only the results for two special wave numbers are given here. First, the photon dispersion relations for wave number parallel to the uniform orientation \mathbf{b} of the defects ($k_z = 0$) are equal for both polarization modes:

$$!^{[\ell=3]} k_{jj}^2 = !^{[\ell=3]} k_{jj}^2 = 1 - 4 nb^3 c^2 k_{jj}^2 + 2 nb^3 d^2 c^2 k_{jj}^4 + \dots ; \quad (\text{A 2})$$

Second, the photon dispersion relations for wave number perpendicular to the defect orientation ($k_{jj} = 0$) are different for the two polarization modes (i.e., show birefringence):

$$!^{[=3]}(0; k_?)^2 = 1 + 8 nb^3 c^2 k_?^2 \quad (8 = 5) nb^5 c^2 k_?^4 + \dots; \quad (\text{A 3a})$$

$$!^{[=3]}(0; k_?)^2 = 1 + 16 nb^3 c^2 k_?^2 + (16 = 5) nb^5 c^2 k_?^4 + \dots; \quad (\text{A 3b})$$

neglecting terms down by a factor of $b \ll d$.

The results of this appendix make clear that birefringence only occurs if there is some kind of "conspiracy" between individual asymmetric defects which are part of the spacetime foam.

APPENDIX B : MODIFIED DIRAC WAVE FUNCTION

In this Appendix, we use the Dirac representation of the matrices (formal signature + and globalinkowski coordinates) and refer to Refs [44, 45, 46] for further details. For simplicity, we also set $c = \hbar = 1$. The Dirac equation in Schrödinger form reads then

$$\not{e}(\mathbf{x}; t) = (\not{\gamma} - \not{\mathbf{r}} + m) \not{\psi}(\mathbf{x}; t); \quad (\text{B 1})$$

with 4 4 matrices

$$\not{\gamma}_0 = \begin{matrix} \not{1}_2 & 0 \\ 0 & \not{1}_2 \end{matrix}; \quad \not{\gamma} = \begin{matrix} 0 & \not{\gamma} \\ \not{\gamma} & 0 \end{matrix}; \quad (\text{B 2})$$

in terms of the 2 2 unit matrix $\not{1}_2$ and the Pauli matrices $\not{\gamma}$.

In the presence of a single $\epsilon = 1$ defect (sphere with radius b centered at $\mathbf{x} = 0$ and antipodal identification), we impose the following boundary condition on the Dirac spinor:

$$(\not{e}(\mathbf{x}; t) = \not{\mathbf{k}} \not{\gamma} \not{\psi}(\mathbf{x}; t); \quad \mathbf{x} \neq \mathbf{0}) \quad (\text{B 3})$$

with unit vector $\not{\mathbf{k}} = \mathbf{x} \not{\mathbf{j}}$. [There can be an additional phase factor $2\pi(j, j=1)$ on the right-hand side of (B 3), which may in principle depend on the direction, $\not{\mathbf{k}} = (\not{\mathbf{k}})$.] The physical motivation of boundary condition (B 3) is that a Dirac particle moves appropriately near the defect at $\not{\mathbf{j}} = b$. Recall that, in the first-quantized theory considered (cf. Ref. [45]), the free particle is described by a wave packet which can in principle have an arbitrarily small extension, for example, much less than b . The boundary condition (B 3) then makes the probability current $\not{\mathbf{j}} = \not{\psi}^\dagger \not{\mathbf{1}}_4 \not{\psi}$ well behaved near the defect at $\not{\mathbf{j}} = b$: probability density j^0 equal at antipodal points, normal component of $\not{\mathbf{j}}$ going through, and tangential components of $\not{\mathbf{j}}$ changing direction (cf. Fig. 1 and the discussion in Sec. II B).

The case of primary interest to us has spin $\frac{1}{2}$ particles of very high energy compared to the rest mass m but wavelength still much larger than the individual defect size b :

$$m \ll k \ll 1/b; \quad (\text{B 4})$$

An appropriate initial solution of the Dirac equation over \mathbb{R}^3 is given by

$$(\mathbf{x}; t)_{\text{in}} = \exp(-kz) \begin{pmatrix} 0 & 1 \\ 1 & 0 \\ \frac{B}{C} & 0 \\ 0 & \frac{C}{A} \end{pmatrix}; \quad (B 5)$$

which corresponds to a positive-energy plane wave propagating in the $z = x^3$ direction. This wave function, however, does not satisfy the defect boundary condition (B 3) for the manifold (2.2) with a single defect centered at $\mathbf{x} = 0$.

Make now the following monopole-like Ansatz for the required correction:

$$(\mathbf{x}; t)_{\text{corr}} = \exp(-!t) g(r=b) \begin{pmatrix} 0 & 1 \\ 1 & s_1 \\ \frac{B}{C} & s_2 \\ \frac{B}{C} & s_3 \\ 0 & A \end{pmatrix}; \quad (B 6)$$

s_4

with radial coordinate $r = \|\mathbf{x}\|$ and normalization $g(1) = 1$. (This particular Ansatz is motivated by the structure of the Green's function for the Dirac operator; cf. Sec. 34 of Ref. [44].) The total wave function,

$$(\mathbf{x}; t) = (\mathbf{x}; t)_{\text{in}} + (\mathbf{x}; t)_{\text{corr}}; \quad (B 7)$$

must then satisfy the defect boundary condition (B 3) at $r = b$, in the limit $kb \rightarrow 0$. The appropriate constant spinor $(s_1; s_2; s_3; s_4)$ in (B 6) is readily found. Also, the function g in the "near zone" ($r \ll b$) must be given by $g(r=b) = b^2 = r^2$, in order to satisfy the Dirac equation neglecting terms of order b, kb , and $m = k$.

All in all, we have for the corrected wave function from a single defect centered at $\mathbf{x} = \mathbf{x}_1$:

$$(\mathbf{x}; t) = \exp(-kz) \begin{pmatrix} 0 & 1 \\ 1 & 0 \\ \frac{B}{C} & 0 \\ 0 & \frac{C}{A} \end{pmatrix} + \exp(-!t) \begin{pmatrix} 0 & 1 \\ 1 & 0 \\ \frac{b^2}{r_1^2} \frac{B}{C} & \frac{\cos_1}{\sin_1} \exp(-!r_1) \\ \frac{\sin_1}{\cos_1} \exp(-!r_1) & \frac{C}{A} \end{pmatrix}; \quad (B 8)$$

where (r_1, θ_1, ϕ_1) are standard spherical coordinates with respect to the defect center \mathbf{x}_1 and the z axis from the globalinkowski coordinate system, having $r_1 = \|\mathbf{x} - \mathbf{x}_1\|$, $\theta_1 \in [0, \pi]$, and $\phi_1 \in [0, 2\pi]$.

Next, sum over the contributions of N identical defects with centers $\mathbf{x} = \mathbf{x}_j$, for $j = 1, \dots, N$. The resulting Dirac wave function is given by

$$(\mathbf{x}; t) = \exp(-kz) \begin{pmatrix} 0 & 1 \\ 1 & 0 \\ \frac{B}{C} & 0 \\ 0 & \frac{C}{A} \end{pmatrix} + \exp(-!t) \sum_{j=1}^{N^2} \frac{1}{\|\mathbf{x} - \mathbf{x}_j\|^2} \begin{pmatrix} 0 & 1 \\ 1 & 0 \\ \frac{B}{C} & \frac{\cos_j}{\sin_j} \exp(-!r_j) \\ \frac{\sin_j}{\cos_j} \exp(-!r_j) & \frac{C}{A} \end{pmatrix}; \quad (B 9)$$

where θ_j and ϕ_j are polar and azimuthal angles with respect to the defect center \mathbf{x}_j and the z axis. With many randomly positioned defects present ($N \gg 1$), the entries of the second spinor on the right-hand side of (B9) average to zero and only the initial Dirac spinor remains.

For the electromagnetic case discussed in Sec. II B, the octupole electric dipoles (radial dependence $1/r^3$) are aligned by the linearly polarized initial electric field (2.8) and there remains a correction field after averaging, which leads to a modification of the photon dispersion relation. As mentioned above, the corrective wave function required for the Dirac spinor is monopole-like (radial dependence $1/r^2$) and averages to zero. This different behavior is, of course, a manifestation of the fundamental difference between vector and spinor fields.

The final result is that the dispersion relation of a high-energy Dirac particle is unchanged, $\omega_p^2 = k^2$, at least up to leading order in $m b$ and $k b$. For an initial spinor wave function at rest ($k = 0$ and $m = 1/b$), a similar calculation gives $\omega_p^2 = m^2$. Combined, we then have for a free Dirac particle (for definiteness, taken to be a proton),

$$\omega_p^2 = m^2 + k^2 + \dots; \quad (B10)$$

to leading order in $m b$ and $k b$.

To summarize, we have found in this appendix that the classical spacetime foam model considered affects the quadratic coefficient of the proton dispersion relation differently than the one of the photon dispersion relation. Remains that the calculation performed here was only in the context of the first-quantized theory and a proper second-quantized calculation is left for the future.

-
- [1] J.A. Wheeler, *Ann. Phys. (N.Y.)* 2, 604 (1957).
- [2] J.A. Wheeler, in: *Battelle Rencontres 1967*, edited by C.M. DeWitt and J.A. Wheeler (Benjamin, New York, 1968), pp. 242–307.
- [3] S.W. Hawking, *Nucl. Phys. B* 144, 349 (1978).
- [4] S.W. Hawking, D.N. Page, and C.N. Pope, *Nucl. Phys. B* 170, 283 (1980).
- [5] J. Friedman, M.S. Morris, I.D. Novikov, F. Echeverria, G. Klinkhamer, K.S. Thorne, and U. Yurtsever, *Phys. Rev. D* 42, 1915 (1990).
- [6] M.V. Visser, *Lorentzian Wormholes: From Einstein to Hawking* (Springer, New York, 1996).
- [7] H.A. Bethe, *Phys. Rev.* 66, 163 (1944).
- [8] E.F. Beall, *Phys. Rev. D* 1, 961 (1970).
- [9] S.R. Coleman and S.L. Adler, *Phys. Lett. B* 405, 249 (1997), [hep-ph/9703240](#).
- [10] G. Almehiri-Camelia, J.R. Ellis, N.E.M.avromatos, D.V. Nanopoulos, and S. Sarkar, *Nature* 393, 763 (1998), [astro-ph/9712103](#).
- [11] M.Nakahara, *Geometry, Topology and Physics* (Institute of Physics Publishing, Bristol, 1990).
- [12] J.D. Jackson, *Classical Electrodynamics*, second edition (Wiley, New York, 1975).

- [13] R.P. Feynman, R.B. Leighton, and M. Sands, *The Feynman Lectures on Physics* (Addison Wesley, Reading, MA, 1963 and 1964), Vols. I and II.
- [14] W.K.H. Panofsky and M. Phillips, *Classical Electricity and Magnetism*, second edition (Addison Wesley, Reading, MA, 1962).
- [15] Higher-order multipoles ($\ell = 3; 5; 7; \dots$) contribute with a factor $b^{\ell+2} [j_{\ell-1}(kb) + j_{\ell+1}(kb)]$ and are, therefore, suppressed by additional powers of b . Note the different letter type used for multipole ℓ and defect separation l .
- [16] L.B. Brillouin, *Wave Propagation and Group Velocity* (Academic, New York, 1960).
- [17] For the analogous problem of bubbly ice mentioned in the Introduction, the scattering of acoustic waves has been discussed by P.B. Price, *Nucl. Instrum. Meth. A* 325, 346 (1993); astro-ph/0506648. Incidentally, the motivation for these studies is the acoustic detection of ultrahigh-energy cosmic neutrinos by a possible extension of the IceCube optical array; see J.A. Vandenbroucke et al., *Int. J. Mod. Phys. A* 21S1, 259 (2006), astro-ph/0512604. Contrary to the case of protons, such cosmic neutrinos would not suffer from vacuum Cherenkov radiation (at least, at tree level) and bounds similar to (4.4) in the main text would not occur.
- [18] R. Lehnert, *Phys. Rev. D* 68, 085003 (2003), gr-qc/0304013.
- [19] F.R. Linkhamer, *Nucl. Phys. B* 578, 277 (2000), hep-th/9912169.
- [20] F.R. Linkhamer and C. Rupp, *Phys. Rev. D* 70, 045020 (2004), hep-th/0312032.
- [21] F.R. Linkhamer and C. Rupp, *Phys. Rev. D* 72, 017901 (2005), hep-ph/0506071.
- [22] F.R. Linkhamer and C. Rupp, to appear in *New. Astron. Rev.*, astro-ph/0511267.
- [23] As mentioned in the last paragraph of Sec. II A, the $\ell = 2$ space is simply connected, which implies that there are no anomalous effects on the photon propagation [19, 20]. But, as shown in Sec. II B, the photon propagation is still modified by taking into account the boundary-condition effects for the standard Maxwell equations.
- [24] J.R. Ellis, K. Farakos, N.E. Mavromatos, V.A. Moutsou, and D.V. Nanopoulos, *Astrophys. J.* 535, 139 (2000), astro-ph/9907340.
- [25] J.R. Ellis, N.E. Mavromatos, D.V. Nanopoulos, A.S. Sakharov, and E.K.G. Sarkisyan, *Astropart. Phys.* 25, 402 (2006), astro-ph/0510172.
- [26] T. Jacobson, S. Liberati, and D. Mattingly, *Ann. Phys. (N.Y.)* 321, 150 (2006), astro-ph/0505267.
- [27] The numerical factor 2 on the right-hand side of Eq. (6.3) in Ref. [20] is wrong and must be replaced by 3=2.
- [28] S.D. Biller et al., *Phys. Rev. Lett.* 83, 2108 (1999), gr-qc/9810044.
- [29] D.J. Bird et al., *Astrophys. J.* 441, 144 (1995), astro-ph/9410067.
- [30] M. Risse, P. Homola, D. Gora, J. Pekala, B. Wilczynska, and H. Wilczynski, *Astropart. Phys.* 21, 479 (2004), astro-ph/0401629.
- [31] O. Gagnon and G.D. Moore, *Phys. Rev. D* 70, 065002 (2004), hep-ph/0404196.
- [32] Bounds (4.4a) and (4.4b) in the main text correspond to the bound (1.9) and the K_1 bound (1.14) of Ref. [31], respectively.
- [33] The only caveat we have regards the calculation of the proton dispersion relation and is stated

in the last sentence of App. B. For this reason, we have employed the parametrization (3.2), which is valid generally, even though the interpretation of the individual scales \bar{b} and \bar{l} may be less transparent than in, for example, Eq. (3.3).

- [34] A. Friedman, *Z. Phys.* **21**, 326 (1924) [*Gen. Rel. Grav.* **31**, 2001 (1999)].
- [35] For completeness, we also mention the rare red-gas interpretation of our results. If somehow the ratio \bar{b}/\bar{l} is very small and saturates $\lim \bar{b}/\bar{l}$ (4.4a), $\bar{b}/\bar{l} \approx 3 \times 10^8$, then $\lim \bar{b}/\bar{l}$ (4.4b) gives $\bar{b} < 9 \times 10^{27} \text{ m}$.
- [36] As a concrete example, take the $\epsilon = 1$ defects of Sec. II A to be time-dependent, with typical lifetime τ and average re-appearance time T . In other words, a single defect with fixed position in space is "on" for a fraction $\tau = T$ of the time and the different defects occupy a fraction $n\bar{b}^3 = \bar{b}^3 = l^3$ of space. (The implicit assumption here is that topology change is allowed; see, e.g., Chap. 6 of Ref. [6] for further discussion.) In a long-wavelength calculation along the lines of Sec. II B, there would then be defects hopping around in the nearly constant electric and magnetic fields of the initial plane wave. For $\tau = T = 2 = 1$ and $\bar{b} = 1$, the octupole moments would be turning on and off rapidly and one naively expects effective permittivities $\epsilon = 1 + 4 F$ and $\epsilon = 1 - 2 F$, with an excluded-space-time-volume factor $F = (\bar{b}/l^3)^2$ ($\tau = T$). The modified dispersion relation would now be $\omega^2 = (1 - 2 F)^2 k^2 + O(k^4)$. If correct, an astrophysics bound similar to (4.4a) applies to $\omega^2 F$ and rules out such a single-scale spacetime foam with $\bar{b} = 1$ $\ll \tau \ll T$.
- [37] Preliminary results on particle propagation in a quantum gravity context have been reported in, e.g., Refs. [4, 38, 39, 40].
- [38] R. Gambini and J. Pullin, *Phys. Rev. D* **59**, 124021 (1999), gr-qc/9809038.
- [39] J. Alfaro, H.A. Morales-Tecotl, and L.F. Uruñuela, *Phys. Rev. D* **65**, 103509 (2002), hep-th/0108061.
- [40] H. Sahlmann and T. Thiemann, *Class. Quant. Grav.* **23**, 909 (2006), gr-qc/0207031.
- [41] The apparent smoothness of space would be even more surprising for so-called TeV gravity models [42, 43], with a "Planck scale" of the higher-dimensional gravity at approximately 10 TeV . In that case, the theorist must explain why TeV ("near-Planckian") gamma rays and ultra-high-energy ("trans-Planckian") cosmic rays propagate with a universal maximum limiting velocity and without sizable dispersion effects, as exemplified by the experimental bounds (4.2), (4.3), and (4.4) in the main text.
- [42] N. Arkani-Hamed, S. Dimopoulos, and G.R. Dvali, *Phys. Lett. B* **429**, 263 (1998), hep-ph/9803315.
- [43] V.A. Rubakov, *Phys. Uspekhi* **44**, 871 (2001) [*Usp. Fiz. Nauk* **171**, 913 (2001)], hep-ph/0104152.
- [44] M.E. Rose, *Relativistic Electron Theory* (Wiley, New York, 1961).
- [45] J.J. Sakurai, *Advanced Quantum Mechanics* (Addison-Wesley, Reading, MA, 1967).
- [46] C. Itzykson and J.-B. Zuber, *Quantum Field Theory* (McGraw-Hill, New York, 1980).